HIGH-FREQUENCY DIFFRACTION BY A STRIP LOCATED AT THE INTERFACE BETWEEN TWO DIFFERENT MEDIA: THE CASE OF H-POLARIZATION

Sevtap Sapmaz*, Kazuya Kobayashi* and Alinur Büyükaksoy**

* Department of Electrical and Electronic Engineering, Chuo University
1-13-27 Kasuga, Bunkyo-ku, Tokyo 112, Japan
** Faculty of Electrical and Electronics Engineering
Technical University of Istanbul, 80626 Maslak, Istanbul, Turkey

1. Introduction

The problem of diffraction by a metallic strip in composite media is an important subject in diffraction theory and it is relevant to several engineering applications. Although electromagnetic diffraction by strips and slits has been extensively studied by several authors following different analytical and numerical methods, almost all works are limited to the case where the strips and slits are located in a homogeneous medium. The diffraction by a slit in a perfectly conducting plane screen between two media has been investigated by Butler and Umashankar [1] based on numerical solutions of integral equations and by Hongo [2] using the Weber-Schafheitlin discontinuous integrals. Van Splunter and van den Berg [3] analyzed the diffraction by a perfectly conducting strip residing in the plane interface between two media using the spectral theory of diffraction. In [4], we have employed the Wiener-Hopf technique to solve the E-polarized plane wave diffraction by the same geometry as in [3], and clarified the secondary diffraction characteristics within the framework of ray optics. In our recent paper [5], we have re-examined the same problem as in [4] to derive lateral wave contributions and uniform asymptotic expressions for the diffracted field.

The purpose of this paper is to analyze the diffraction problem involving the same geometry as in [4,5] for H-polarization and compare the high-frequency diffraction characteristics with the results of the case of E-polarization. Applying the boundary conditions to the integral representations for the unknown scattered field, the problem is formulated in terms of the modified Wiener-Hopf equation (MWHE), which is reduced to a pair of simultaneous integral equations via the factorization and decomposition procedure. The method of successive approximations is then applied, and the first, second and third order asymptotic solutions of the integral equations are derived explicitly for the strip width large compared with the wavelength. Taking the inverse Fourier transform and applying the saddle point method, the high-frequency scattered far field expression is derived. Illustrative numerical examples of the bistatic radar cross section (RCS) are presented and the far field scattering characteristics are discussed in detail by comparing with the results of the case of E-polarization. Since the solution technique is similar to that for the E-polarized case [4,5], the analytical details will be omitted in the following.

The time factor is assumed to be $e^{-i\omega t}$ and suppressed throughout the paper.

2. Wiener-Hopf Analysis of the Problem

The geometry of the problem is shown in Fig. 1, where $u^i(\equiv H_z^i)$ is the incident plane wave of H-polarization, and the perfectly conducting strip occupies the region $\{(x,y,z)|\ 0<x<l,\ y=0,\ z\in(-\infty,\infty)\}$. The upper ($y>0$) and lower ($y<0$) media are characterized by the relative permittivity/permeability (ε_1,μ_1) and (ε_2,μ_2), respectively. The wave numbers for the regions $y>0$ and $y<0$ are denoted by $k_1(=\omega\sqrt{\varepsilon_1\mu_1})$ and $k_2(=\omega\sqrt{\varepsilon_2\mu_2})$, respectively.

Let the total magnetic field $u^T(x,y)\ [\equiv H_z^T(x,y)]$ be

$$u^T(x,y)=u^s(x,y)+\begin{cases} u^i(x,y)+Re^{-ik_1(x\cos\theta_0-y\sin\theta_0)}, & y>0 \\ Te^{-ik_2(x\cos\theta_1+y\sin\theta_1)}, & y<0 \end{cases} \tag{1}$$

with

$$u^i(x,y)=e^{-ik_1(x\cos\theta_0+y\sin\theta_0)},\qquad \theta_0\in(0,\pi/2) \tag{2}$$

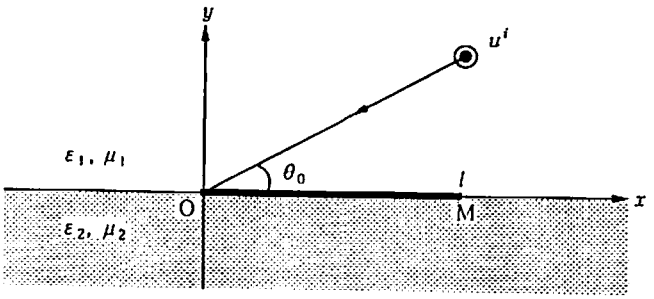

Fig. 1. Geometry of the problem.

$$R = \frac{\varepsilon_2 k_1 \sin\theta_0 - \varepsilon_1 k_2 \sin\theta_1}{\varepsilon_2 k_1 \sin\theta_0 + \varepsilon_1 k_2 \sin\theta_1}, \qquad T = R + 1 \tag{3}$$

In Eqs. (1) and (3), θ_1 is the transmission angle defined by $k_1 \cos\theta_0 = k_2 \cos\theta_1$. Our problem is to solve the two-dimensional Helmholtz equation for the scattered field $u^s(x,y)$ by enforcing the boundary conditions as well as the radiation and edge conditions. For convenience of analysis, we assume the media to be slightly lossy as in $k_{1,2} = \mathrm{Re}(k_{1,2}) + i\mathrm{Im}(k_{1,2})$ with $0 < \mathrm{Im}(k_1) < \mathrm{Im}(k_2) \ll \mathrm{Re}(k_{1,2})$.

In view of the radiation condition, $u^s(x,y)$ is expressed by using the unknown spectral coefficients $A(\alpha)$ and $B(\alpha)$, as in

$$u^s(x,y) = \begin{cases} \displaystyle\int_{-\infty+ic}^{\infty+ic} A(\alpha) e^{i\nu_1(\alpha)y - i\alpha x} d\alpha, & y > 0 \\ \displaystyle\int_{-\infty+ic}^{\infty+ic} B(\alpha) e^{-i\nu_2(\alpha)y - i\alpha x} d\alpha, & y < 0 \end{cases} \tag{4}$$

with $|c| < \mathrm{Im}(k_1)$, where $\nu_{1,2}(\alpha) = \sqrt{k_{1,2}^2 - \alpha^2}$ with $\mathrm{Im}\,[\nu_{1,2}(\alpha)] > 0$. Taking into account the boundary conditions on the strip and the material interface, the problem is formulated in terms of the modified Wiener-Hopf equation (MWHE) satisfied by the unknown functions $P(\alpha)$ and $F_\pm(\alpha)$ as in

$$\frac{P(\alpha)}{K(\alpha)} + F_-(\alpha) + e^{i\alpha l} F_+(\alpha) = \frac{T}{2\pi i} \frac{\varepsilon_1}{\varepsilon_2} k_2 \sin\theta_1 \frac{e^{il(\alpha - k_1\cos\theta_0)} - 1}{\alpha - k_1 \cos\theta_0} \tag{5}$$

for $|\mathrm{Im}(\alpha)| < \mathrm{Im}(k_1)$, where

$$A(\alpha) = B(\alpha) = -\frac{P(\alpha)}{K(\alpha)}, \quad K(\alpha) = \frac{\varepsilon_1}{\nu_1(\alpha)} + \frac{\varepsilon_2}{\nu_2(\alpha)} \tag{6}$$

$$F_-(\alpha) = \frac{1}{2\pi} \int_{-\infty}^{0} u^s(x, +0) e^{i\alpha x} dx \tag{7a}$$

$$F_+(\alpha) = \frac{1}{2\pi} \int_{l}^{\infty} u^s(x, +0) e^{i\alpha(x-l)} dx \tag{7b}$$

$$P(\alpha) = \frac{1}{2\pi} \int_{0}^{l} J_z^{(e)}(x) e^{i\alpha x} dx \tag{7c}$$

It follows from the radiation condition that $F_+(\alpha)$ and $F_-(\alpha)$ are regular in the upper ($\mathrm{Im}(\alpha) > \mathrm{Im}(-k_1)$) and lower ($\mathrm{Im}(\alpha) < \mathrm{Im}(k_1)$) halves of the complex α-plane, respectively, while $P(\alpha)$ is an entire function. The function $J_z^{(e)}(x)$ corresponds to the surface current on the strip.

Applying the factorization and decomposition procedure, the MWHE is reduced to a pair of simultaneous integral equations. The integral equations are solved asymptotically for large strip width via the method of successive approximations leading to the first, second and third order solutions. The high-frequency scattered far field expression is derived by taking the inverse Fourier transform and applying the saddle point method. The results show that the first order solution leads to the geometrical optics field, the singly diffracted field and the lateral waves, while the second and third order solutions correspond to the doubly and triply diffracted fields, respectively. It should be noted that the diffracted field in our analysis is uniformly valid in incidence and observation angles.

3. Illustrative Results and Discussion

In this section, we shall present numerical examples of the bistatic RCS to discuss the far field scattering characteristics of the strip. Let (ρ, ϕ) and (r, ψ) be cylindrical coordinates defined by $x = \rho\cos\phi$, $y = \rho\sin\phi$ and $x - l = r\cos\psi$, $y = r\sin\psi$ for $-\pi < \phi < \pi$ and $-\pi < \psi < \pi$. Figures 2 and 3 are numerical results of the bistatic RCS as a function of observation angle $\phi(\approx \psi)$, where σ/λ denotes the normalized RCS for the total scattered field and σ_n/λ for $n = 2$ and 3 denote the normalized RCS for the second and third order scattered fields, respectively, with λ being the free-space wavelength. We have also plotted the results for the E-polarized case [5] to enable comparison between two different polarizations. In these examples, the strip width l is 10λ, and the incidence angle θ_0 has been fixed as 45°. The relative permittivity ϵ_1, ϵ_2 and the relative permeability μ_1, μ_2 for numerical computations are $\epsilon_1 = 1.2248$, $\epsilon_2 = \mu_1 = \mu_2 = 1.0$ in Fig. 2, and $\epsilon_2 = 1.2248$, $\epsilon_1 = \mu_1 = \mu_2 = 1.0$ in Fig. 3.

We see from the figures that main lobes for the total scattered field are located at $\phi = 135°, -141°$ in Fig. 2(a) and $\phi = 135°, -130°$ in Fig. 3(a). It is clear that the peaks at $\phi = 135°$ and $\phi = -141°, -130°$ correspond to the shadow boundaries of the reflected and transmitted waves, respectively. On comparing the characteristics of the second and third order scattered fields for E and H polarizations in Figs. 2(b), 2(c), 3(b) and 3(c), the maximum level of the bistatic RCS for the second and third order scattered fields for the E-polarized case is about 25 dB and 55 dB lower than that for the H-polarized case, respectively. The second and third order scattered fields correspond to the doubly and triply diffracted fields, respectively and hence, it is inferred that the effect of the higher order scattering depends on inverse powers of $k_{1,2}l$. Carrying out non-uniform asymptotic expansions, we can show that the second and third order scattered fields are, respectively, $O\left((k_{1,2}l)^{-3/2}\right)$ and $O\left((k_{1,2}l)^{-5/2}\right)$ for the E-polarized case and $O\left((k_{1,2}l)^{-1/2}\right)$ and $O\left((k_{1,2}l)^{-3/2}\right)$ for the H-polarized case, as $k_{1,2}l \to \infty$. If we compare the results for E and H polarizations, we see that the higher order scattered fields for E-polarization are $1/l$ times weaker than that for H-polarization. We shall now make somewhat more detailed investigation on the higher order scattering characteristics. It is observed from Figs. 2(b) and 2(c) that the bistatic RCS for the second and third order scattered fields gives spurs at $\phi = 25.4°$ and 154.6°, which are shown to coincide precisely with the calculated values of the critical angles of the total reflection. It is therefore confirmed that the higher order scattered field is affected by the lateral waves. The spurs at $\phi = -25.4°, -154.6°$ in Figs. 3(b) and 3(c) may be interpreted in the same manner as above.

Acknowledgment

This work was supported in part by the Institute of Science and Engineering, Chuo University.

References

[1] Butler, C. M. and Umashankar, K. R., *Radio Sci.*, vol. 11, no. 7, pp. 611-619, July 1976.

[2] Hongo, K., *Trans. IECE Japan*, vol. 55-B, no. 1, pp. 25-26, Jan. 1972 (in Japanese).

[3] van Splunter, J. M. and van den Berg, P. M., *Can. J. Phys.*, vol. 57, no. 8, pp. 1148-1156, 1979.

[4] Büyükaksoy, A. and Uzgören, G., *Radio Sci.*, vol. 22, no. 2, pp. 183-191, Mar.-Apr. 1987.

[5] Sapmaz, S., Kobayashi, K., Büyükaksoy, A. and Uzgören, G., *IEICE Trans. Electron.*, vol. E79-C, 1996, to be published.

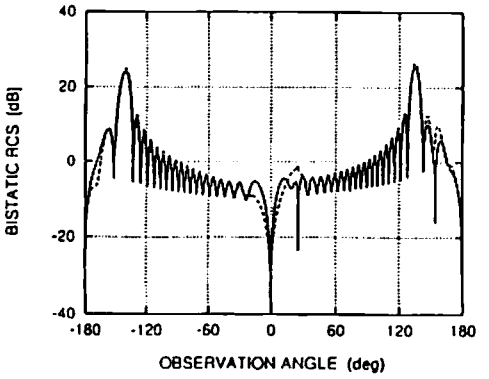

(a) σ/λ (total scattered field).

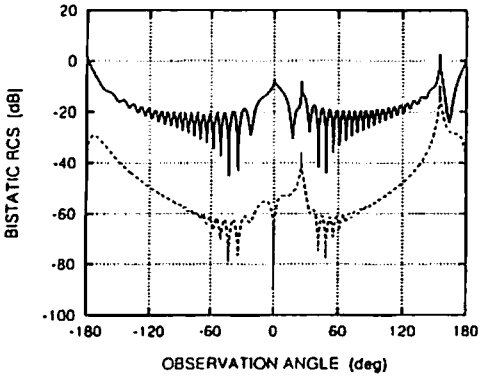

(b) σ_2/λ (second order scattered field).

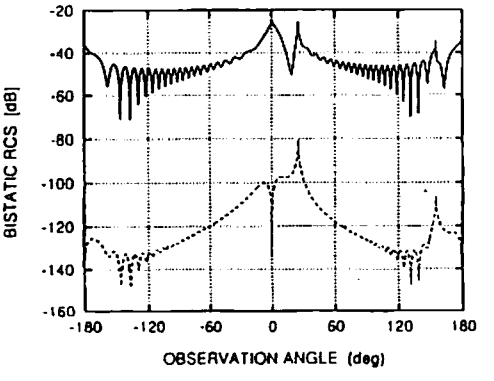

(c) σ_3/λ (third order scattered field).

Fig. 2. Bistatic RCS for
$(\varepsilon_1, \mu_1)=(1.2248,1)$, $(\varepsilon_2, \mu_2)=(1,1)$.
Solid and dashed lines denote the results
for H and E polarizations, respectively.

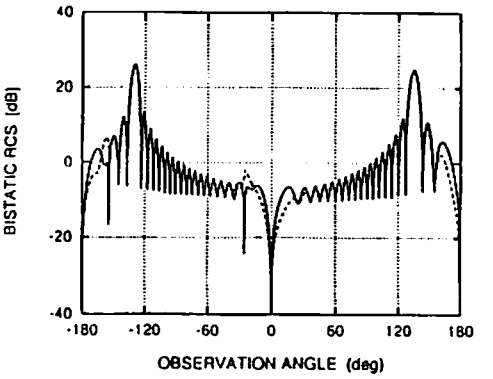

(a) σ/λ (total scattered field).

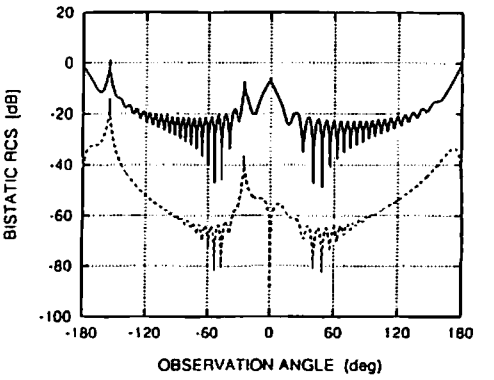

(b) σ_2/λ (second order scattered field).

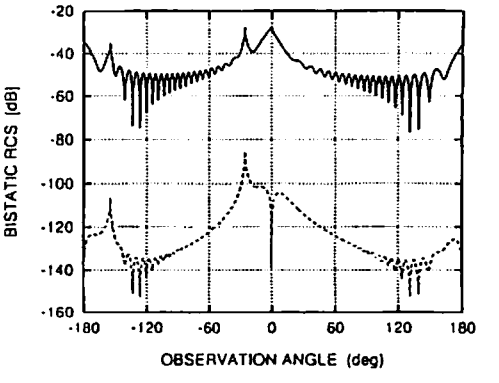

(c) σ_3/λ (third order scattered field).

Fig. 3. Bistatic RCS for
$(\varepsilon_1, \mu_1)=(1,1)$, $(\varepsilon_2, \mu_2)=(1.2248,1)$.
Solid and dashed lines denote the results
for H and E polarizations, respectively.